

Isomer Spectroscopy in $^{216}\text{Th}_{126}$ and the Magicity of $^{218}\text{U}_{126}$

K. Hauschild,¹ M. Rejmund,^{2,*} H. Grawe,² E. Caurier,³ F. Nowacki,³ F. Becker,^{1,†} Y. Le Coz,¹ W. Korten,¹ J. Döring,² M. Górska,² K. Schmidt,² O. Dorvaux,^{4,‡} K. Helariutta,^{4,§} P. Jones,⁴ R. Julin,⁴ S. Juutinen,⁴ H. Kettunen,⁴ M. Leino,⁴ M. Muikku,^{4,||} P. Nieminen,⁴ P. Rähkila,⁴ J. Uusitalo,⁴ F. Azaiez,⁵ and M. Bellegric^{5,¶}

¹DAPNIA/SPhN CEA Saclay, F-91191 Gif-sur-Yvette, France

²Gesellschaft für Schwerionenforschung, Planckstrasse 1, D-64291 Darmstadt, Germany

³IReS, F-67037 Strasbourg Cedex 2, France

⁴Accelerator Laboratory, University of Jyväskylä, P.O. Box 35, FIN-40351, Finland

⁵IPN, F-91406 Orsay Cedex, France

(Received 9 May 2001; published 25 July 2001)

Excited states in ^{216}Th were investigated via prompt and delayed γ decays and the recoil-decay tagging method. The decay schemes of the $I^\pi = (8^+)$, $t_{1/2} = 128(8) \mu\text{s}$, the $I^\pi = (11^-)$, $t_{1/2} = 615(55) \text{ ns}$, and the $I^\pi = (14^+)$, $t_{1/2} \geq 130 \text{ ns}$ isomers were established. The configuration $\pi h_{9/2} f_{7/2}$ is assigned to the $I^\pi = (8^+)$ isomer, which implies that the $h_{9/2}$ and $f_{7/2}$ states are nearly degenerate. This is ascribed to increased binding of the $f_{7/2}$ orbital by its coupling to a low-lying $I^\pi = (3^-)$ state at $E_x = 1687 \text{ keV}$. The role of octupole and pairing correlations for a $Z = 92$ shell closure prediction is discussed on the basis of shell model calculations.

DOI: 10.1103/PhysRevLett.87.072501

PACS numbers: 27.80.+w, 21.10.Pc, 23.20.Lv, 23.60.+e

The shell stabilization of the superheavy elements is determined by the single particle structure, normally taken from mean field predictions [1]. The comparison to experimental data is masked by the existence of correlations, which are not treated in standard mean field calculations. In contrast, the spherical shell model contains all correlations in the effective interaction, as deduced from nucleon-nucleon potentials by G -matrix many-body theory [2,3]. The propagation of the single particle energies from a well-studied magic nucleus, such as ^{208}Pb , into the open shell is limited by the model space even in the largest available shell model codes. We have chosen the region beyond ^{208}Pb , the heaviest and best known doubly magic shell closure for an experimental study of these complementary approaches.

Recent systematic mean field calculations for superheavy elements [1] predict a substantial shell gap for $Z = 92$, $N = 126$ (^{218}U), i.e., between the proton $h_{9/2}$ and $f_{7/2}$ single particle orbitals. This is at variance with an extrapolation of single quasiparticle energies from the lighter $N = 126$ isotones known up to ^{215}Ac [4]. However, the positions of the $f_{7/2}$ and $i_{13/2}$ orbitals can be highly distorted by octupole correlations which are not considered in the standard mean field approach. For example, in ^{208}Pb [5,6] an additional 130- and 264-keV binding was found for the corresponding $g_{9/2}$ and $j_{15/2}$ orbitals, respectively. The study of single particle energies and octupole correlations in ^{216}Th , the two-hole nucleus in the predicted proton subshell closure, could shed light on these controversial predictions, and provides a stringent test of the predictive power of mean field calculations at high Z . With the development of large scale shell model codes nearly untruncated calculations have become possible for ^{216}Th , which will probe the realistic interactions derived for the best known shell model core ^{208}Pb [2,7].

Detailed γ -ray spectroscopy of ^{216}Th is hampered by low production cross sections ($\sim 40 \mu\text{b}$) due to fission competition and the existence of a $t_{1/2} \sim 180 \mu\text{s}$ high-spin isomer detected by its $\sim 3\%$ α -decay branch [8]. In the present study the powerful technique of recoil-decay tagging (RDT) [9,10] was used to isolate the ^{216}Th channel by exploiting the characteristic properties of the ground state α decay of ^{216}Th .

Excited states in ^{216}Th were populated in two separate experiments performed at the Accelerator Laboratory of the University of Jyväskylä. In the first experiment, a self-supporting 0.5 mg/cm^2 -thick natural Hf target was bombarded with a $185 \text{ MeV } ^{40}\text{Ar}$ beam producing ^{216}Th via the fusion-evaporation reaction $^{180}\text{Hf}(^{40}\text{Ar}, 4n)^{216}\text{Th}$. In the second, similar experiment the $^{172}\text{Yb}(^{48}\text{Ca}, 4n)^{216}\text{Th}$ reaction was performed with a 0.97 mg/cm^2 -thick self-supporting target enriched to 94.9% in ^{172}Yb and a beam energy of 217 MeV . Data were collected for 50 h.

In the second experiment γ -ray data were measured at both the target and focal plane positions. Prompt γ rays, emitted at the target position, were detected in the JURO-SPHERE II array [11] which consisted of 26 Compton-suppressed Ge detectors. At the focal plane five Compton-suppressed Ge detectors were used to measure delayed γ rays emitted from the deexcitation of isomeric states. The total photopeak efficiencies of the arrays were $\sim 1.7\%$ and $\sim 0.7\%$ at 1.3 MeV , respectively.

The recoiling fusion-evaporation residues were separated in flight magnetically from the background of primary beam and fission fragments by the gas-filled recoil separator RITU [12]. The separated ions were then stopped in a 16-strip position-sensitive Si detector situated at the focal plane of RITU. The subsequent position- and time-correlated α decays, characteristic of the implanted recoils, were also measured in the Si detector. To distinguish both

α -decay events from scattered particles and fusion products from scattered beam events a multiwire proportional gas counter was positioned 110 mm upstream of the Si detector.

Data were recorded with the condition that the focal plane Si detector fired starting coincidence time windows of (a) 1 μ s, corrected for the recoil time of flight, during which prompt γ rays at the target position were recorded, and (b) 32 μ s during which delayed γ rays emitted at the focal plane were recorded. All events were labeled by a continuous time stamp with a precision of 1 μ s. This allowed temporal correlations between recoil and α events to be determined during data analysis.

An α -particle energy of 7.919(6) MeV was obtained for the ground state α decay of ^{216}Th from $N_\alpha = 52\,308(312)$ decays. The ground state half-life of ^{216}Th was determined to be $t_{1/2} = 25.4(8)$ ms using the method described in Ref. [13]. These results are consistent with previously measured values summarized in Ref. [14]: $E_\alpha = 7.921(8)$ MeV and $t_{1/2} = 28(2)$.

For the known isomeric state in ^{216}Th , $E_\alpha = 9.915(15)$ MeV and $t_{1/2} = 128(8)$ μ s were obtained ($N_\alpha = 750$). These values also compare favorably to the previously measured values of $E_\alpha = 9.933(15)$ MeV and $t_{1/2} = 140(5)$ μ s [14]. This places the isomeric state at an excitation energy of 2.032(15) MeV with the assumption that the isomeric state α decays directly to the ground state of the daughter.

In the subsequent data analysis, position-correlated recoil ^{216}Th α events observed within a maximum time interval of 250 ms were selected. In Figs. 1(a) and 1(b) we present γ -ray transitions observed, in coincidence with ^{216}Th α particles position correlated with recoils, at the target and focal plane positions, respectively. The time difference between recoil implantation and the detection of individual γ rays at the focal plane greatly facilitated the placement of delayed γ rays in the level scheme. Restricting the time difference between the recoil implantation and the detection of a delayed γ ray to <3.65 μ s enhances the 150-, 466-, 517-, 607-, and 883-keV transitions; see Fig. 1(c). In contrast, requiring that the delayed γ ray was observed after 3.65 μ s of the recoil implantation isolates the 126-, 200-, 209-, and 1478-keV transitions; see Fig. 1(d). Individual γ gates set in a recoil gated α tagged delayed γ - γ matrix suggest that the 126-, 200-, 209-, and 1478-keV transitions are mutually coincident. The sum of these individual gates is shown in Fig. 1(e).

Efficiency corrected intensities for the 126-, 200-, 209-, and 1478-keV cascade transitions show a deficiency for the 200-keV γ ray, which amounts to only 70(14)% of the average 126- and 209-keV intensity (see Table I). This can be consistently explained by electron conversion only by assigning multipolarity $E1$ for the 209- and 126-keV lines, and $E2$ for the 200-keV line. On the basis of $N = 126$ systematics shown in Fig. 2 the 1478-keV line is identified with the $(2^+) \rightarrow 0^+$ transition. In contrast to the delayed

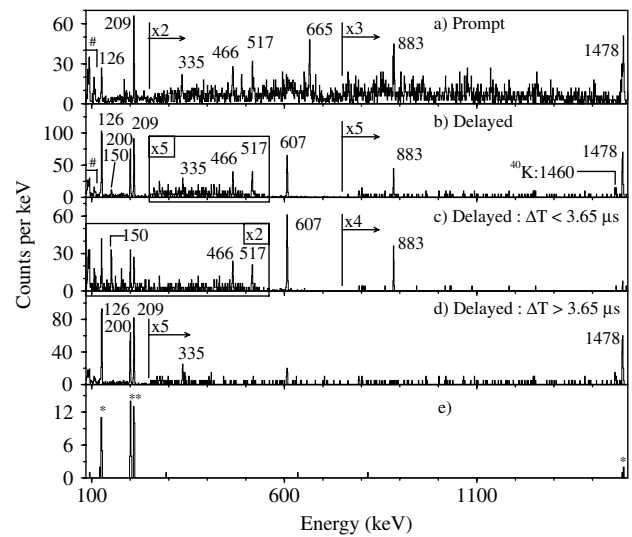


FIG. 1. ^{216}Th γ -ray energy spectra obtained using the RDT correlation technique with a 250 ms search time. Ge singles spectra observed at (a) the target position, and (b) the RITU focal plane. Delayed Ge singles spectra obtained with recoil-implantation γ -ray time differences (c) less than 3.65 μ s, and (d) greater than the 3.65 μ s. (e) Coincidence spectrum obtained from a sum of gates, indicated with an asterisk, on a delayed $\gamma\gamma$ matrix. Transition energies are labeled in keV. Th x rays are labeled with an “#.”

γ -ray spectrum of Fig. 1(b) there is little evidence of a 200-keV line in the prompt spectrum of Fig. 1(a). The 200-keV transition is therefore placed above the 126- and 209-keV transitions. The 126-keV transition is placed above the 209-keV line from similar intensity arguments based on the prompt γ -ray spectrum. The weak 335-keV line observed in Figs. 1(a), 1(b), and 1(d) is interpreted as a stretched $E2$ transition decaying in parallel to the 126- and 209-keV transitions.

The delayed γ rays of 150, 883, and 607 keV have been placed on top of the $I^\pi = (8^+)$ isomer following the $N = 126$ systematics in Fig. 2. The 607-keV line has been found to decay with $t_{1/2} = 615(55)$ ns, which is ascribed to a $I^\pi = (11^-)$ $E3$ isomer. For the 150–883-keV cascade only a limit of $t_{1/2} \geq 130$ ns can be deduced, due to its low intensity. It is based on the assumption that the intensity

TABLE I. γ -ray transitions associated with the 8^+ isomer in ^{216}Th observed at the focal plane: γ -ray energies E_γ , efficiency corrected relative intensities I_γ , efficiency and electron conversion corrected relative intensities, and most probable transition multipolarities σL .

E_γ (keV)	I_γ (%)	$I_\gamma(1 + \alpha_{\text{TOT}})$			
		$E1$	$E2$	$M1$	σL
1478	74(14)	74(14)	<u>74(14)</u>	74(14)	$E2$
209	100(16)	<u>106(17)</u>	157(25)	344(55)	$E1$
126	100(12)	<u>119(13)</u>	305(37)	721(87)	$E1$
200	70(7)	77(8)	<u>117(12)</u>	263(26)	$E2$

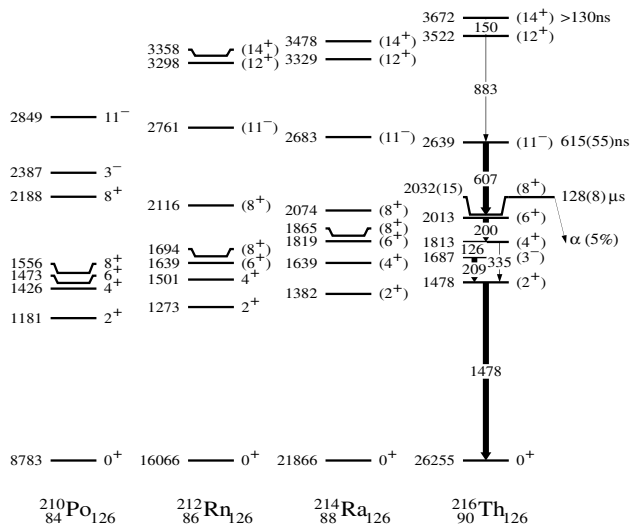


FIG. 2. Level scheme for ^{216}Th , deduced from the delayed γ rays observed in the present work, compared with other $N = 126$ isotones. Excitation and ground state binding energies relative to ^{208}Pb are given in keV.

reduction relative to the 607-keV line to 7(2)% is due to decay losses in flight only.

Additional γ rays, which could not be placed in the level scheme due to poor coincidence statistics, were observed delayed in the focal plane: 466 and 517 keV, and prompt at the target: 466, 517, and 665 keV.

In Fig. 3 and Table II the experimental level scheme of ^{216}Th and the deduced γ -ray transition strengths are compared to results of two shell model approaches. First, an empirical shell model (ESM) calculation for pure configurations was performed with single particle energies, residual interaction, and effective $E2$ and $E3$ operators taken from the ^{208}Pb neighbors ^{209}Bi and ^{210}Po . Second, a shell model calculation was performed in the $\pi(h_{9/2}, f_{7/2}, i_{13/2}, p_{3/2}, f_{5/2}, p_{1/2})$ model space beyond $Z = 82$, using the realistic Kuo-Herling [2] interaction as modified by Brown and Warburton [7] (KHBW), and using a proton polarization charge of $\delta e_\pi = 1.0e$.

From the $N = 126$ systematics (Fig. 2) two 8^+ states with stretched configurations $h_{9/2}^2$ and $h_{9/2}f_{7/2}$ are expected at near degeneracy below a $h_{9/2}i_{13/2}$, $I^\pi = 11^-$ isomer. The $I^\pi = 11^-$ isomer is expected to decay via an enhanced $E3$ to the $h_{9/2}f_{7/2}$ 8^+ level since the branch to the $h_{9/2}^2$ 8^+ state is extremely weak due to its spin-flip character (see Table II). The decay half-life of the γ rays below the $I^\pi = (8^+)$ isomer were determined to be $t_{1/2}(8^+:\gamma) = 90(70) \mu\text{s}$ in the short observation interval of 32 μs . Therefore we conclude that the α -decay branch [$t_{1/2} = 128(8) \mu\text{s}$] originates from the same isomer as the unobserved highly converted $8^+ \rightarrow 6^+$ $E2$ transition of $E_\gamma = 19(15) \text{keV}$. The γ -branching ratio is $95_{-5}^{+3}\%$, which is to be compared to the value of 97% estimated in previous work [8]. Because of the nonobservation of the weak $E3$ branch and of the highly converted $M1$ and

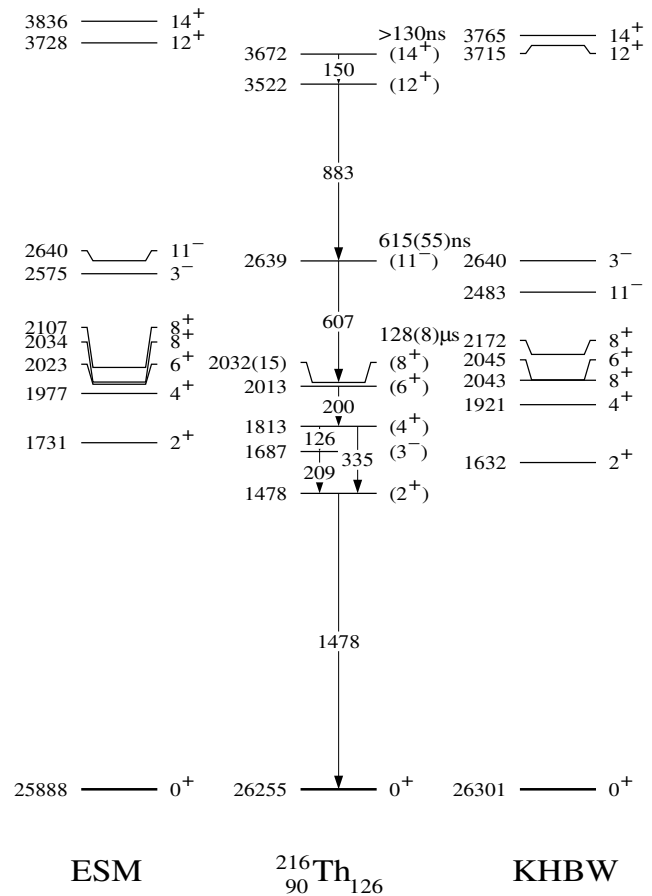


FIG. 3. Experimental level scheme for ^{216}Th compared with empirical (ESM) and full shell model calculations (KHBW).

$E2$ transitions connecting the two 8^+ states to each other and to the 6^+ state at 2013 keV, the relative positions of the 8^+ states cannot be inferred firmly from the present data. The experimental limit $0.043e^2 \text{fm}^4 \leq B(E2; 8^+ \rightarrow 6^+) \leq 0.77e^2 \text{fm}^4$ favors an $h_{9/2}f_{7/2}$ assignment to the observed isomer yielding small $B(E2)$ values (Table II) in both models. An $h_{9/2}^2$ assignment would greatly exceed the experimental upper limit. Placing the $h_{9/2}^2$ state below the 6^+ state would form an yrast trap and imply a long-lived α decay estimated to be $t_{1/2} > 1.2 \text{ms}$ from the partial half-life of the observed α branch. Such a long-lived α decay is not observed [14], and we suggest that the two configurations have swapped positions.

The lowering of the $f_{7/2}$ state can be explained by the strong $L = 3$ vibrational coupling to the close-lying $i_{13/2}$ orbit as manifest in the dramatically decreasing position of the 3^- state from 2.615 MeV in ^{208}Pb to 1.687 MeV in ^{216}Th (Fig. 2). This behavior was predicted in an earlier analysis of the $\nu j_{15/2} \rightarrow \nu g_{9/2}$ $E3$ transitions in the $N = 127$ isotones [15]. An estimate in the spirit of a similar calculation for the ^{208}Pb neighbors [6] yields shifts of -772 and -527keV for the $f_{7/2}$ and $i_{13/2}$ states, respectively. This will close the $h_{9/2}-f_{7/2}$ shell gap. Unfortunately, the enhanced $E3$ ground state transition from the

TABLE II. Experimental vs theoretical γ -ray transition strengths for yrast isomers in ^{216}Th . Configurations are labeled relative to $^{218}\text{U}_{126}$ with seniority ν as subscript.

I_i^π	I_f^π	σL	EXP (Wu) ^a	Leading Configurations	ESM (Wu)	KHBW (Wu)
(8 ⁺)	(6 ⁺)	$E2$	0.0017_{-11}^{+83}	$h_1^{-3}f \rightarrow h_2^{-2}$ $h_2^{-2} \rightarrow h_2^{-2}$	0.00013 1.08	0.050 0.088
(11 ⁻)	(8 ⁺)	$E3$	21(2)	$h_1^{-3}i \rightarrow h_1^{-3}f$ $h_1^{-3}i \rightarrow h_2^{-2}$	13.8 0.137	10.2 0.586
(14 ⁺)	(12 ⁺)	$E2$	<0.245	$h_3^{-3}f \rightarrow h_3^{-3}f$	2.38	0.424

^aWeisskopf units $B_W(E2) = 76.99e^2 \text{fm}^4$ and $B_W(E3) = 1414.06e^2 \text{fm}^6$.

1687-keV state could not be observed at the present detection limits, due to the $E1$ competition.

It is obvious that the shell model calculation (KHBW) cannot account for the $L = 3$ correlations determining the position of the 3^- state and $E3$ transition strength (Fig. 3 and Table II). Except for this deficiency, which is due to the omission of excitations of the $Z = 82$, $N = 126$ core, the agreement obtained for levels and transition strengths is remarkable. Especially the ground state binding energies listed in Figs. 2 and 3 and the trend of the 2^+ energies and high-spin states is perfectly reproduced throughout the sequence of $N = 126$ isotones [16]. In support of the experimental conclusions the predictions for the $Z = 91-94$, $N = 126$ isotones do not show any sign of a shell gap at $Z = 92$.

At first sight the results from the empirical (ESM) and the large scale (KHBW) shell model calculation shown in Fig. 3 seem to agree well with each other and experiment. However, a closer inspection of wave functions and transition strengths also reveals substantial differences.

(i) The retardation of the $(h_{9/2}f_{7/2})_{8^+} \rightarrow (h_{9/2}^2)_{6^+}$ $E2$ strength in both models is due to the $f_{7/2} \rightarrow h_{9/2}$ spin-flip $E2$ matrix element.

(ii) The small $B(E2)$ within the seniority $\nu = 2$ $(h_{9/2})^n$ multiplet in the full calculation is due to the reduced occupation of the $h_{9/2}$ orbital with only 4–6 particles, while the rest is scattered in pairs to the $f_{7/2}$ and $i_{13/2}$ orbitals. This produces a typical retarded midshell $B(E2)$ [4] in contrast to the well-established seniority schemes in intruder high-spin orbitals such as $\pi g_{9/2}$ in $N = 50$, $\pi \nu h_{11/2}$ in $Z = 50$, and $N = 82$ and $\nu i_{13/2}$ in $Z = 82$ semimagic nuclei. The ESM assumes a pure $(h_{9/2})^8$ wave function and neglecting pairing yields a much larger $B(E2)$.

(iii) The KHBW calculation predicts the $(h_{9/2})^n$, 8^+ state to be an yrast trap in contrast to experimental evidence as discussed above, while the ESM clearly places the $(h_{9/2}f_{7/2})_{8^+}$ to be yrast.

In summary, the isomer spectroscopy of ^{216}Th has revealed a number of isomers with simple shell model configurations and a low-lying $I^\pi = (3^-)$ state. A large scale shell model calculation and an empirical shell model analysis of the experimental data give evidence for strong pairing and/or $L = 3$ correlations. This counteracts the

existence of a $Z = 92$ shell gap as predicted in mean field calculations and calls for the need to include these correlations in the mean field approach. From the $N = 126$ systematics of even nuclei (Fig. 2) it is inferred that the 2^+ and 3^- states swap positions in ^{218}U . Accordingly the ground state of ^{217}Pa may be expected to be an $f_{7/2}$ state.

The staff at JYFL is thanked for providing excellent beam and technical support. This work was supported by the Access to Large Scale Facility program under the Training and Mobility of Researchers (TMR) program of the European Union.

*Present address: DAPNIA/SPHn CEA Saclay, F-91191 Gif-sur-Yvette, France.

†Present address: GANIL, BP 5027, 14076 Caen Cedex 5, France.

‡Present address: IReS, F-67037 Strasbourg Cedex 2, France.

§Present address: Laboratory of Radiochemistry, 00014 University of Helsinki, Finland.

||Present address: Daresbury Laboratory, Warrington, WA4 4AD Cheshire, U.K.

¶Present address: University of Surrey, Guildford GU2 7XH, U.K.

- [1] K. Rutz *et al.*, Nucl. Phys. **A634**, 67 (1998).
- [2] T. T. S. Kuo and G. H. Herling, NRL Memorandum Report No. 2258, 1971.
- [3] M. Hjorth-Jensen *et al.*, Phys. Rep. **261**, 125 (1995).
- [4] D. J. Decman *et al.*, Z. Phys. A **310**, 55 (1983).
- [5] I. Hamamoto, Phys. Rep. **10**, 63 (1974).
- [6] M. Rejmund *et al.*, Eur. Phys. J. A **8**, 161 (2000).
- [7] E. K. Warburton and B. A. Brown, Phys. Rev. C **43**, 602 (1991).
- [8] R. Hingmann *et al.*, Nucl. Phys. **A404**, 51 (1983).
- [9] R. S. Simon *et al.*, Z. Phys. A **325**, 197 (1986).
- [10] E. S. Paul *et al.*, Phys. Rev. C **51**, 78 (1995).
- [11] R. Julin, Acta Phys. Pol. B **28**, 269 (1997).
- [12] M. Leino *et al.*, Nucl. Instrum. Methods Phys. Res., Sect. B **99**, 653 (1995); M. Leino, *ibid.* **126**, 320 (1997).
- [13] M. Leino *et al.*, Phys. Rev. C **24**, 2370 (1981).
- [14] F. P. Hessberger *et al.*, Eur. Phys. J. A **8**, 521 (2000).
- [15] G. Dracoulis *et al.*, Nucl. Phys. **A493**, 145 (1989).
- [16] E. Caurier *et al.*, in Proceedings of SM2K [Nucl. Phys. A (to be published)].